Design of Peptidomimetics That Inhibit the Association of Phosphatidylinositol 3-Kinase with Platelet-Derived Growth Factor-β Receptor and Possess Cellular Activity

Scott R. Eaton, Wayne L. Cody,* Annette M. Doherty, Debra R. Holland, Robert L. Panek,† Gina H. Lu,† Tawny K. Dahring,† and David R. Rose‡

Departments of Chemistry and Vascular and Cardiac Diseases, Parke-Davis Pharmaceutical Research, Division of Warner-Lambert Company, Ann Arbor, Michigan 48105, and Department of Medicine, University of California at San Diego, Whittier Diabetes Program, Veteran's Administration Research Foundation, 9500 Gilman Drive, La Jolla, California 92093

Received May 4, 1998

Phosphorylated tyrosine residues of growth factor receptors that associate with intracellular proteins containing src-homology 2 (SH2) domains are integral components in several signal transduction pathways related to proliferative diseases such as cancer, atherosclerosis, and restenosis. In particular, a phosphorylated pentapeptide [pTyr^{751}-Val-Pro-Met^{754}-Leu (pTyr = phosphotyrosine)] derived from the primary sequence of platelet-derived growth factor-β (PDGF-β) receptor blocks the association of the C-terminal SH2 domain of the p85 subunit of phosphatidylinositol 3-kinase (PI 3-kinase) to PDGF-β receptor with an IC_{50} of 0.445 ± 0.047 μM. Further evaluation of the structure−activity relationships for pTyr^{751}-Val-Pro-Met-Leu resulted in the design of smaller peptidomimetics with enhanced affinity including Ac-pTyr-Val-Ala-N(C_6H_{13})$_2$ (IC_{50} = 0.076 ± 0.010 μM). In addition, the phosphotyrosine residue was replaced with a difluorophosphonate derivative [4-phosphono(difluoromethyl)phenylalanine (CF_2Pmp)] which has been shown to be stable to cellular phosphatases. The extracellular administration of either CF_2Pmp-Val-Pro-Met-Leu or Ac-CF_2Pmp-Val-Pro-Met-NH_2 in a whole cell assay resulted in specific inhibition of the PDGF-stimulated association from the C-terminal SH2 domain of the p85 subunit of PI 3-kinase to the PDGF-β receptor in a dose-dependent manner. These compounds were also effective in inhibiting GLUT4 translocation, *c-fos* expression, and cell membrane ruffling in single-cell microinjection assay.

Introduction

The proliferation, differentiation, and survival of normal cells are regulated by a variety of extracellular signaling mitogens known as growth factors. These polypeptidic growth factors include epidermal growth factor (EGF), fibroblast growth factors (FGFs), and platelet-derived growth factor (PDGF). Growth factors have been implicated in numerous disease states involving uncontrolled cellular proliferation and differentiation, including cancer, atherosclerosis, and restenosis.[1−3] In clinical studies, restenosis [i.e., the angiographic reocclusion of the arterial wall following percutaneous transluminal coronary angioplasty (PTCA, or better know as balloon angioplasty)] occurs in 20−45% of patients within the first 3−6 months following treatment.[4−6] In this report, a unique approach to the prevention of restenosis utilizing peptidomimetics designed to block intracellular signaling pathways mediating cellular proliferation and differentiation will be described.

Both the FGFs and PDGF are potent vascular smooth muscle cell (VSMC) mitogens and chemoattractants.[7] The migration and proliferation of VSMCs are an initial and critical step in the onset of restenosis following balloon angioplasty. In fact, after balloon injury to rat carotid arteries an upregulation of PDGF and FGF receptor isoforms has been observed. In this model, the infusion of PDGF following arterial damage resulted in an increase of VSMC migration along with a corresponding increase in thickening of the neointimal layer.[8,9] However, antibodies raised to PDGF significantly inhibited this process.[10]

Upon the binding of PDGF to its extracellular receptor, dimerization of the receptor occurs followed by autophosphorylation of several tyrosines on intracellular protein substrates and/or the receptor, itself. These phosphorylated tyrosines act as high-affinity binding sites for several cellular proteins involved in signal transduction pathways which are linked to cellular proliferation.[2,11−13] One such protein is phosphatidylinositol 3-kinase (PI 3-kinase). PI 3-kinase is 1 of more than 20 cytosolic proteins involved in intracellular signaling that contain src-homology (SH2) domains. SH2 domains consist of approximately 100 amino acids that are highly conserved across other such cytosolic proteins and possess high-affinity binding sites for specific phosphorylated tyrosines of growth factor receptors.[2,11−13] In particular, it has been shown that a significant increase in DNA synthesis occurs in NMuMG cells when PDGF receptors are specifically associated with PI 3-kinase.[14] Thus, the intracellular blockade of the association of PDGF with PI 3-kinase should have therapeutic implications for the modulation of restenosis and other proliferative diseases mediated by growth factor receptors.

* To whom correspondence should be addressed. Phone: (734) 622-7729. Fax: (734) 622-3107. E-mail: Wayne.Cody@wl.com.
† Vascular and Cardiac Diseases, Parke-Davis Pharmaceutical Research.
‡ University of California at San Diego.

10.1021/jm9802766 CCC: $15.00
Published on Web 09/26/1998

PI 3-kinase is a heterodimeric enzyme that contains a noncatalytic 85-kDa (p85) subunit and a catalytic 110-kDa (p110) subunit.[15,16] The p85 subunit consists of one SH3 and two SH2 domains (N- and C-terminal) that bind specifically to phosphorylated tyrosines on activated growth factor receptors.[17] Of the two SH2 domains the C-terminal SH2 domain, like the full-length p85, distinguishes between the wild-type and a mutant PDGF receptor that lacks the PI 3-kinase binding site. Thus, the C-terminal SH2 domain of the p85 subunit of PI 3-kinase (p85 C-SH2) accounts for the high-affinity binding of PI 3-kinase to PDGF-β receptor.[18] This report will concentrate on the inhibition of this interaction.

As previously discussed, several cytosolic proteins contain SH2 domains. Several high-affinity phosphorylated small peptides and peptidomimetic inhibitors of src[19−24] and, more recently, grb2[25] SH2 domains have been discovered or designed through library approaches[19,20] and systematic rational drug design strategies.[21−25] Previous successes in the systematic rational design of high-affinity and selective peptides/peptidomimetics for src[21−24] prompted us to initiate a similar approach for inhibition of the association of p85 C-SH2 with PDGF-β receptor.

In particular, it has been shown that PI 3-kinase specifically associates with pTyr^{740} (pTyr = phosphotyrosine) and pTyr^{751} of the PDGF-β receptor. In fact, it has been shown that pentapeptides corresponding to these phosphotyrosines [pTyr^{740}-Met-Asp-Met-Ser (**1**) and pTyr^{751}-Val-Pro-Met-Leu (**2**)] were able to inhibit 90% of the in vitro association of PDGF-β receptor with p85 C-SH2 at a concentration of 100 μM.[14] In subsequent studies, it was determined that compound **2** has an IC_{50} of 0.445 ± 0.04 μM for inhibiting this association.[26−28] [In our hands, pTyr^{740}-Met-Asp-Met-Ser (compound **1**) possessed an IC_{50} of 0.522 ± 0.12 μM. However, further structure−activity relationship (SAR) studies utilizing rational drug design strategies were performed on compound **2**, since this compound was conformationally constrained with a proline residue in its primary sequence and additional structural data was also available.[26]] Further analysis of compound **2** revealed that several modifications were well-tolerated for the Val (pY + 1), Pro (pY + 2), and Leu (pY + 4) residues. However, the pTyr (pY) and Met (pY + 3) residues were intolerant of even minimal modification.[26]

The X-ray crystal structures of phosphorylated peptides containing the pTyr-Glu-Glu-Ile motif bound to both the src[29] and lck[30] SH2 domains have been reported. Both of these structures were highly similar and further emphasized the importance of the molecular interactions of pTyr (pY) and Ile (pY + 3) for high-affinity binding. In both cases, an arginine residue was found at the base of the phosphotyrosine binding pocket (pY) that formed a bidentate ion-pairing interaction with the phosphate group, and the isoleucine was completely buried in a hydrophobic binding pocket (pY + 3). The remaining residues were extended across the surface of the protein and through a network of hydrogen bonds that held the pY and pY + 3 residues in their respective binding pockets. Essentially, the mode of binding is best described as a two-pronged model.

In addition, the X-ray crystal structures of phosphoundecapeptides encompassing pTyr^{740} and pTyr^{751} of PDGF-β receptor bound to the N-terminal SH2 domain of p85 of PI 3-kinase (p85 N-SH2) have been reported.[31] Both of these structures were highly similar to those reported for phosphopeptides binding to the src[29] and lck[30] SH2 domains, further supporting a two-pronged binding model for phosphopeptides to SH2 domains.[31] Recently, a crystal has been obtained for a phosphorylated pentapeptide bound to p85 C-SH2 of human PI 3-kinase which diffracted to 1.7 Å, although specific structural data was not provided.[32]

The proton NMR structure of Ac-pTyr^{751}-Val-Pro-Met-Leu bound to p85 C-SH2 has been reported and further highlights the molecular interactions observed in the X-ray crystallographic studies.[33] Basically, the pY and pY + 3 pockets were seen to be occupied by the phosphotyrosine and methionine of the above substrate, respectively, with the remainder of the residues lying across the surface of the protein. In addition, a heteronuclear NMR study of the association of a synthetic 12-amino acid, phosphopeptide that encompasses pTyr^{751} to p85 N-SH2 further supports the importance of these interactions. This solution-phase NMR study revealed that few conformational changes were observed in the protein except for those residues that were directly associated with the pY and pY + 3 binding pockets.[34] Therefore, the X-ray crystallographic and homonuclear and heteronuclear NMR results were consistent with a two-pronged binding model for phosphopeptides to SH2 domains. Herein, we will discuss how these observations, together with homology molecular modeling, were exploited in the design of peptidomimetic inhibitors of the association of p85 C-SH2 with PI 3-kinase.

It has been shown that the inhibition of the association of PDGF-β receptor with the p85 C-SH2 can be achieved with synthetic phosphopeptides and that this may provide a novel approach to the treatment of restenosis; however, several concerns need to be addressed. These include the following: (a) the stability of peptide/peptidomimetic compounds to exo- and/or endopeptidases, (b) the stability of phosphorylated tyrosine-containing compounds to intracellular phosphatases, (c) the ability to deliver the drug candidate to the point of injury, (d) the ability of peptides containing a highly charged phosphate group to be permeable to the cellular membrane, and (e) the ability to specifically inhibit the association of PDGF-β receptor with PI 3-kinase given the number of cytosolic proteins containing SH2 domains. The potential to address and circumvent these concerns with the peptidomimetics reported herein will be discussed and evaluated.

Results and Discussion

A phosphorylated pentapeptide corresponding to the PDGF-β receptor sequence of pTyr^{751}-Val-Pro-Met^{754}-Leu (compound **2**) has been shown to inhibit the association of PDGF-β receptor with p85 C-SH2 of PI 3-kinase in vitro.[14] Specifically, an IC_{50} of 0.445 ± 0.047 μM has been determined for this pentapeptide for the specific blockade of the association of the phosphorylated PDGF-β receptor tyrosine kinase with [^{35}S]GST p85 C-SH2 fusion protein (Table 1).[26−28] In addition, compound **2** has been shown to be selective for the p85 C-SH2 domain over that of src and abl (Table 1).

Table 1. Binding Affinities of Synthetic Compounds **1**−**23** (R1-pTyr-R2-R3-R4) to p85, src, and abl SH2 Domains

compd no.	R1	R2	R3	R4	p85 C-SH2 ± SEM[a] (*n*)[b]	src[a]	abl[a]
1	H	Met	Asp	Met-Ser	0.522 ± 0.12 (2)	ND	ND
2	H	Val	Pro	Met-Leu	0.445 ± 0.047 (16)	12.7	60%[c]
3	H	Val	Pro	Met	6.85 ± 3.26 (2)	ND	ND
4	Ac	Val	Pro	Met-Leu	0.18	5.9	ND
5	H	Val	Pro	Met-Leu-NH_2	0.40	ND	ND
6	Ac	Val	Pro	Met-Leu-NH_2	0.16	ND	ND
7	H	Val	Pro	Met-NH_2	0.485 ± 0.225 (3)	ND	ND
8	Ac	Val	Pro	Met-NH_2	0.264 ± 0.029 (14)	ND	ND
9	H	Val	Pro	Nle-Leu	1.36 ± 0.22 (16)	>10	ND
10	Ac	Val	Ala	*N*-BuGly-NH_2	2.5	ND	ND
11	Ac	Val	Ala	NHC_5H_{11}	16.1 ± 3.4 (3)	ND	ND
12	Ac	Val	D-Ala	NHC_5H_{11}	4.56 ± 1.64 (3)	ND	ND
13	Ac	Val	D-Ala	$N(C_5H_{11})_2$	3.32 ± 0.99 (4)	2.7	25.7
14	Ac	Val	Ala	$N(C_5H_{11})_2$	0.22	1.4	ND
15	Ac	Val	D-Ala	$N(C_4H_9)_2$	5.7	12.5	7.4
16	Ac	Val	Ala	$N(C_4H_9)_2$	0.478 ± 0.129 (3)	5.7	ND
17	Ac	Val	D-Ala	$N(C_6H_{13})_2$	2.5	3.5	6.0
18	Ac	Val	Ala	$N(C_6H_{13})_2$	0.076 ± 0.010 (3)	1.0	5.0
19	Ac	Val	D-Ala	$N(C_8H_{17})_2$	3.47 ± 0.48 (4)	6.1	95.9
20	Ac	Val	Ala	$NH(CH_2)_2C_6H_5$	37.6 ± 8.6 (3)	8.6	46.2
21	Ac	Val	D-Ala	$NH(CH_2)_2C_6H_5$	>100	17.8	72.0
22	Ac	Val	Ala	$NH(CH_2)_2C_6H_{11}$	19.0 ± 1.2 (3)	5.0	26
23	Ac	Val	D-Ala	$NH(CH_2)_2C_6H_{11}$	>100	18.4	ND

[a] IC_{50} values in micromolar concentrations ± standard error of the mean. ND, not determined. [b] n = number of determinations if greater than 1 determination. [c] Percent inhibition at a concentration of 100 μM.

Initial SAR studies were directed at determining the minimal pharmacophore that would inhibit this association. Thus, simple truncation of compound **2** by removing the C-terminal Leu resulted in a greater than 15-fold loss of affinity (compound **3**).[26−28] Interestingly, it was observed that individual or combined neutralization of the amino and carboxy termini was shown to enhance the affinity of compound **2**. For example, N-terminal acetylation (compound **4**) resulted in a 4-fold enhancement of affinity for p85 SH2, while C-terminal amidation (compound **5**) enhanced the affinity ~1.5-fold with respect to compound **2**. Although these modifications were not shown to be additive, N-terminal acetylation and C-terminal amidation of the parent pentapeptide resulted in a very potent analogue (compound **6**) with an IC_{50} of 0.16 μM.[26−28] Interestingly, the neutralization of the amino and carbox termini seems to be a general theme for the design of highly potent inhibitors of several SH2 domains, including src,[19−24] grb2,[25] and p85.[26−28]

The SAR observed in this pentapeptide series was directly translatable to the truncated tetrapeptide series, such that C-terminal amidation led to a 14-fold enhancement in affinity (compound **7** versus compound **3**). Likewise, N-terminal acetylation and C-terminal amidation resulted in a further 2-fold enhancement of affinity (compound **8**, $IC_{50} = 0.264 \pm 0.029$ μM). Thus, the minimal pharmacophore required for inhibiting the association of PDGF-β receptor with p85 C-SH2 was defined by Ac-pTyr-Val-Pro-Met-NH_2.[26−28]

As previously discussed, the SAR,[19,20,26−28] X-ray crystallographic,[29−32] and homonuclear[33] and heteronuclear NMR[34] studies of phosphorylated peptides encompassing Tyr^{751} thru Met^{754} of the PDGF-β receptor sequence have implicated the importance of both residues for high-affinity association with p85 C-SH2 in a two-pronged binding mode. In fact, the only substitution that is readily tolerated for methionine was norleucine.[26,27,35] In particular, this pseudoisosteric substitution resulted in only a 3-fold loss of affinity (compound **9**) with respect to the parent molecule (compound **2**).[26,27,35]

Since neither the proton NMR or X-ray crystallographic structures were available at the time of this study, homology-based molecular modeling was intiated to prepare a theoretical model of p85 C-SH2 domain (Figure 4). As observed for other related SH2 domain structures,[36] the model suggests that the ligand binding surface of p85 C-SH2 is characterized by two distinct pockets: the so-called pY and pY + 3 pockets. The pY pocket is highly electropositive, comprised of two arginine and two serine residues which coordinate with the phosphate oxygens. One of these two arginines, located on the surface of the pY pocket, is also available to interact with an N-terminal group, such as an acetyl. The model also suggested a wide, shallow hydrophobic pY + 3 pocket into which both the pY + 1 and pY + 3 inhibitor residues bind. This characteristic correlates with the reported preference of p85 C-SH2 for peptide sequences of the type pTyr-Hyd-Xxx-Hyd,[19] where Hyd represents a hydrophobic residue and Xxx represents any residue. The pY + 3 pocket is comprised of a phenylalanine, two valines, a leucine, and a cysteine residue. In addition, hydrophobic residues (proline, phenylalanine, valine, and the aliphatic side chain of glutamine) form a shallow channel on the surface of the protein which extends the hydrophobic pY + 3 pocket in a direction away from the pY pocket (Figure 4).

In retrospect, a comparison of this homology model with the later published proton NMR solution structure of p85 C-SH2 complexed to the peptide Ac-pTyr-Val-Pro-Met-Leu[33] does reveal some differences in the protein backbone and side-chain orientations. However, the key features of the model's ligand binding region used for the inhibitor design work described herein are shared by the proton NMR structure: (1) the pY pocket is comprised of the same electrostatically charged residues, (2) the pY + 3 pocket is comprised of the same hydrophobic residues and is approximately the same size, (3) the distance between pY and pY + 3 pockets is

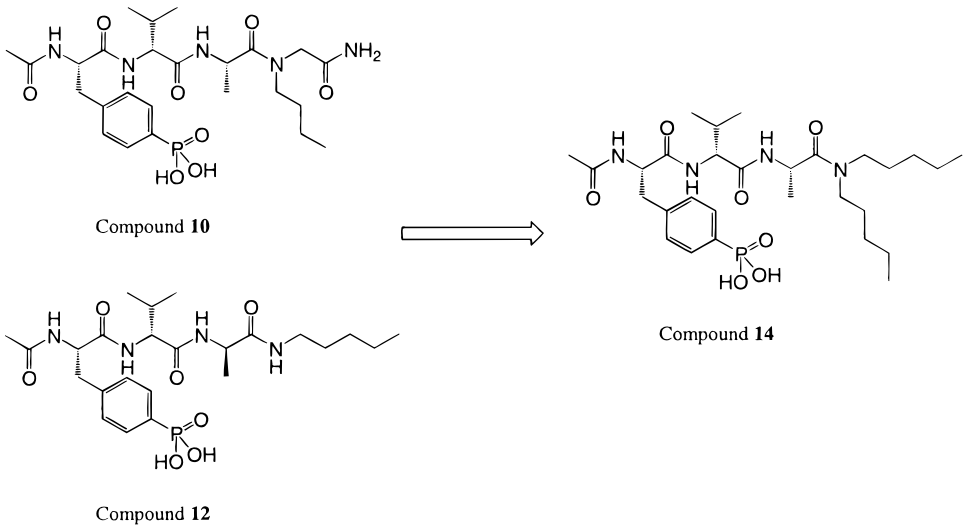

Figure 1. Design of the peptidomimetic dialkylamide series from the peptoid (compound **10**) and the monoalkylamide (compound **12**).

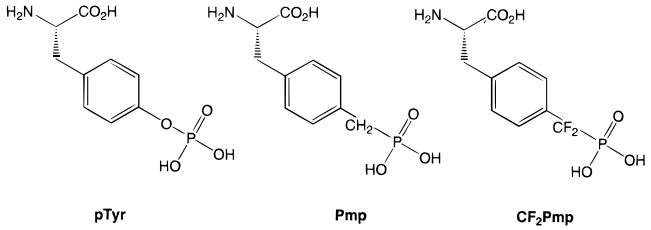

Figure 2. Structures of phosphotyrosine (pTyr), 4-phosphonomethylphenylalanine (Pmp), and 4-phosphono(difluoromethyl)phenylalanine (CF_2Pmp).

approximately the same (~12 Å), and (4) a significant hydrophobic channel does exist in the proton NMR structure as predicted by the model, although this channel as seen in the proton NMR structure is much less solvent-exposed than in our model. This observation might help explain the increased potency of the dialkyl inhibitors described below (Figure 4b). Thus, overall, this homology model, although somewhat different from the later published experimental structure, did predict the key features critical to successful inhibitor design.

Utilizing this homology-based model for p85 C-SH2, it was suggested that transposition of the side chain of methionine and/or norleucine to the amide nitrogen should be a well-tolerated modification while still effectively utilizing the pY + 3 pocket. This "peptoid"[37] (N-alkylated glycine) was efficiently prepared by a solid-phase approach. Initially, bromoacetic acid was coupled to a Rink amide [4-(2′,4′-dimethoxyphenyl-Fmoc-aminomethyl)phenoxyacetamido-norleucylaminomethyl]resin,[38,39] followed by nucleophilic displacement of the bromine with *N*-butylamine, and normal solid-phase peptide synthetic strategies (see the Experimental Section). The peptoid corresponding to compound **2** [Ac-pTyr-Val-Pro-*N*-BuGly-NH_2 (*N*-BuGly = *N*-butylglycine)] was not prepared since this peptoid would be prone to synthetic difficulties such as diketopiperazine formation, premature resin cleavage, and chain termination due to the proline residue adjacent to the *N*-BuGly residue. It was previously reported that pTyr-Val-Ala-Met-Leu possessed an IC_{50} of 2.7 μM,[26] which was only approximately 5-fold less

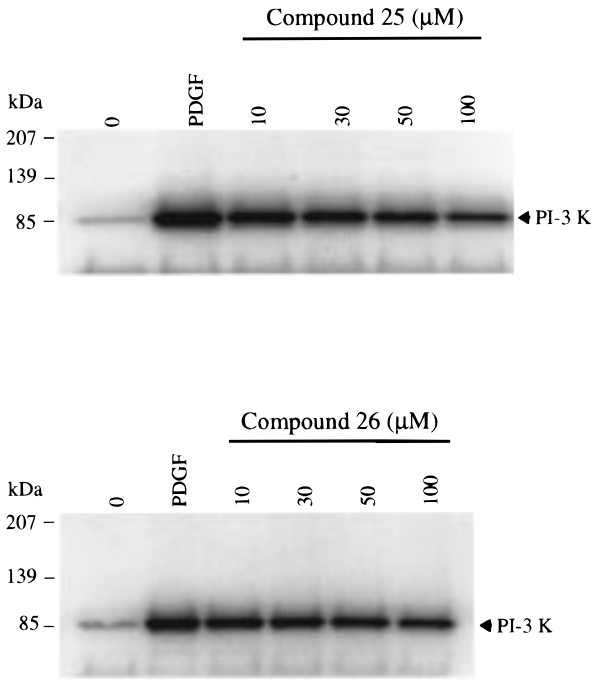

Figure 3. Immunoblot analysis showing the effects of compounds **25** and **26** on the association of the 85-kDa subunit of PI 3-kinase with immunoprecipitated PDGF-β receptors from rat aortic smooth muscle cells. After a 24-h incubation of cells with various concentrations of compound, PDGF-BB (30 ng/mL) was added to cells to stimulate PDGF receptor phosphorylation and the subsequent association of PI 3-kinase. PDGF receptors were immunoprecipitated with PDGF receptor polyclonal antibodies directed against the β-receptor isoform and Western blotted with anti-rat PI 3-kinase polyclonal antibody.

potent than its corresponding proline-containing parent peptide (compound **2**). Therefore, the analogous peptoid corresponding to this sequence was prepared (Ac-pTyr-Val-Ala-*N*-BuGly-NH_2). In addition, molecular modeling also suggested the Ala for Pro substitution, since proline might not allow the necessary binding conformation for the ligand. In fact, the peptoid (compound **10**, Figure 1) possessed an IC_{50} of 2.5 μM. This IC_{50} was within a factor of 10 with respect to the parent tetrapeptide (compound **8**). Thus, it can be postulated that the majority of affinity lost for compound **10** may

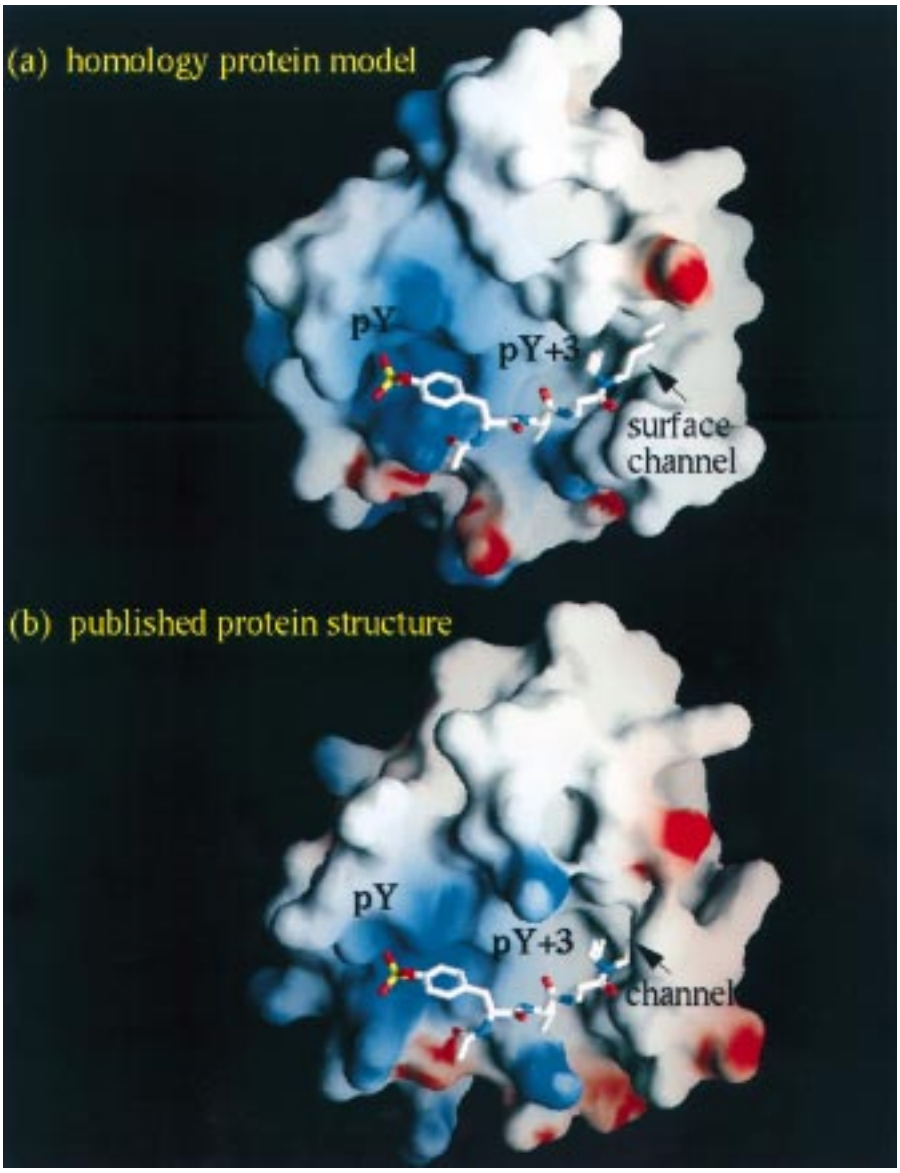

Figure 4. Comparison of the solid molecular surfaces for (a) the p85 C-SH2 homology-based model and (b) the published p85 C-SH2 NMR solution structure.[33] Color coding for the surfaces represents electrostatic potential: red is negative, and blue is positive. In both panels, peptide **14** is shown as a stick figure in the conformation docked into the homolgy model (a). The electropositive pY pocket, hydrophobic pY + 3 pocket, and hydrophobic channel are identified for each molecular surface. Atoms of the inhibitor are colored as red, oxygen; blue, nitrogen; yellow, phosphorus; white, carbon. This figure was prepared using the program GRASP.[71]

be the result of the alanine for proline substitution due to the increased flexibility in the molecule and that, in fact, the peptoid modification was very well-tolerated.

In an effort to design first-generation peptidomimetics, it was observed that a C-terminal carboxylate was detrimental to activity in the tetrapeptide series, while norleucine was well-tolerated as a substitution for methionine. Therefore, it was postulated and supported by modeling that the C-terminal amino acid was replaced with an alkyl chain, such as *N*-pentylamine (Table 1). This modification could be simply incorporated by the preparation of Ac-Tyr(Bzl)-Val-Ala on a Sasrin resin [2-methoxy-4-alkoxybenzyl alcohol (a resin highly susceptible to acidic cleavage conditions)],[40,41] which was cleaved with 1.0% trifluoroacetic acid (TFA) in dichloromethane (DCM) to yield the free carboxylate. The remaining solution-phase synthesis of the target compound consisted of coupling of the amine to the C-terminal carboxylate, deprotection of the tyrosine, phosphorylation, oxidation, deprotection of the phosphorylated tyrosine, and final purification. In principle, this approach should have been effective. Unfortunately, the coupling of *N*-pentylamine to Ac-Tyr(Bzl)-Val-Ala in the presence of 1-(3-dimethylamiopropyl)-3-ethylcarbodiimide hydrochloride (EDCI) and *N*-hydroxybenzotriazole (HOBt) resulted in extensive racemization (∼40−50%) of the C-terminal alanine. However, these diastereoisomers were separable by reversed-phase high-pressure liquid chromatography (RP-HPLC). The major diastereoisomer corresponded to the L-enantiomer of Ala. Ac-pTyr-Val-Ala-NHC_5H_{11} (compound **11**, Figure 1) showed approximately 65-fold less affinity (IC_{50} = 16.1 ± 3.4 μM) than the parent tetrapeptide. However, interestingly the D-Ala-containing analogue (compound **12**) exhibited an IC_{50} of 4.56 ± 1.64 μM. Once again, this binding would be comparable to the parent peptide if the 4−5-fold loss of affinity was a result of the proline to alanine substitution. Despite this loss of

potency, this modification is significant in that it should impart stability against exopeptidases, such as carboxypeptidase, to the molecule.

The design of a second-generation peptidomimetic series resulted from molecular modeling suggesting that the pY + 3 substitution of the peptoid and the C-terminus of the peptidomimetic (compounds **10** and **12**, Figure 1) could be combined into one molecule via a dialkylamide. It was envisioned that this modification would allow interaction with the pY + 3 pocket of p85 C-SH2 via one alkyl chain which is normally occupied by methionine or norleucine, while the second alkyl chain would have further interactions with the hydrophobic channel of the protein surface (Figure 4). [In retrospect, the published NMR structure of p85 C-SH2 suggests that the second alkyl chain would indeed interact with such a hydrophobic surface channel but more extensively than would have been predicted by the homology model since that channel is much less solvent-exposed in the NMR structure (Figure 4b).[33]] Thus, Ac-pTyr-Val-D-Ala-N(C_5H_{11})$_2$ (compound **13**) was prepared using the same synthetic strategy used to prepare compounds **11** and **12**. This compound had an IC_{50} of 3.32 ± 0.99 μM and was essentially equipotent to the parent peptoid and peptidomimetic. However, as seen for the preparation of compound **11**, significant racemization of the C-terminal alanine had occurred. Surprisingly, upon separation by RP-HPLC and evaluation of the L-amino acid-containing isomer (compound **14**, Figure 1), this analogue exhibited an IC_{50} of 0.22 μM for inhibition of the association of the PDGF-β receptor with p85 C-SH2.

It was very interesting and unexpected that the SAR differed between the monoalkyl- and dialkylamides with respect to the stereochemistry of the pY + 2 residue. Previously, it has been shown that utilization of *O*-(7-azabenzotriazol-1-yl)-1,1,3,3-tetramethyluronium hexafluorophosphate (HATU) as a coupling agent, in the presence of 1*H*-hydroxy-7-azabenzotriazole (HOAt), greatly reduced the amount of racemization of the C-terminal amino acid.[42,43] Even though, compounds **17** and **18** were initially prepared racemic and then separated by RP-HPLC (method B in the Experimental Section); they were also synthesized using the HATU/HOAt coupling strategy to verify the stereochemical assignments (method C in the Experimental Section). Indeed, the independent preparation of compounds **17** and **18** by method C confirmed that the stereochemical assignment of the C-terminal alanine was correct and that a reverse in the SAR between the monoalkyl- and dialkylamide series was observed.

To further optimize the activity of these amides, the ideal length of the dialkyl chain was determined. Shortening the chain by one carbon (dibutyl) with both D- and L-alanine in the pY + 2 position (compounds **15** and **16**) led to a modest loss in affinity in both cases (~1.5−2-fold) with respect to the parent dipentylamides. However, increasing the length of the dialkyl chain by one carbon (dihexyl) led to an enhancement of affinity for both the D- and L-alanine cases (compounds **17** and **18**). In fact, compound **18**, is the most potent compound reported to date for inhibiting the association p85 C-SH2 to PDGF-β receptor (IC_{50} of 0.076 ± 0.010 μM). Further extension of the C-terminal dialkyl chain with dioctylamine resulted in a significant loss of affinity (compound **19**, IC_{50} = 3.47 ± 0.48 μM). Thus, the dihexyl chain is optimal for maximum affinity, presumably since each side chain makes optimal contacts with the pY + 3 pocket and the surface channel (Figure 4).

(Interestingly, during the course of this study, it was reported that C-terminal alkylamides are effective substitutions in ligands that bind to src[21−24] and grb2[25] SH2 domains. It was originally suggested in an X-ray crystallography paper[23] and confirmed in a later publication[24] highlighting the SAR of a series of dipeptidomimetic inhibitors of the src SH2 domain that a dipentylamide represented the optimal C-terminal group. In this case, the dipentylamide was slightly better than the dihexylamides and significantly better than the diheptylamides. These results further point to the great similarity between SH2 domains of different proteins and the potential problems in developing compounds selective for a specific SH2 domain.)

Further attempts to optimize the C-terminal amides by the incorporation of phenethyl and cyclohexylethyl resulted in compounds that were essentially inactive (compounds **20**−**23**) which is consistent with the p85 C-SH2 model. However, in both cases, the L-alanine-containing analogues were still more potent than the corresponding D-alanine-containing analogues. Thus, the SAR observed for these compounds is consistent with the dialkylamide series.

Selectivity of Synthetic Compounds for Various SH2 Domains. To develop inhibitors of SH2 domains that may have therapeutic utility for the treatment of restenosis and proliferative diseases, it is critical to design compounds that are selective for p85 C-SH2 over other SH2 domains. In this regard, several of the synthetic analogues were evaluated for their affinity to inhibit the association of the SH2 domains of src and abl. For inhibitors of src, it has been shown that an acidic residue is preferred in the position pY + 1,[19−24] while for the p85 C-SH2 domain a hydrophobic residue, such as valine, is preferred in this position.[14,19,20,26−28] In addition, the native peptide binding sequence for the src SH2 domain contains an isoleucine residue in the pY + 3 position,[19−24] while ligands for the p85 C-SH2 domain contain a methionine residue.[14,19,20,26−28]

For compound **2**, moderate selectivity for the p85 C-SH2 domain over both the src and abl SH2 domains (> 28-fold) was observed. Compound **4** showed greater selectivity for p85 C-SH2 of 33-fold versus the src SH2 domain. Interestingly, the pseudoisosteric replacement of Nle for Met in compound **2** (compound **9**) led to a modest loss of affinity for p85 C-SH2, but this ligand completely lacked affinity for src. Perhaps this is not that surprising since src can accommodate branched amino acids in the pY + 3 pocket.

In the peptidomimetic series, some of the selectivity for src appeared to be diminished. However, compounds containing an L-Ala residue in the pY + 2 position maintained selectivity over those containing the D-Ala residue. For example, compound **13** (D-Ala) showed little difference in preference between p85 C-SH2 and src, but in compound **14** (L-Ala) some selectivity was observed (6-fold). Interestingly, compound **13** did exhibit 8-fold selectivity versus abl. In addition, compound **15** exhibited minimal selectivity for p85 C-SH2

Table 2. Binding Affinities of Synthetic Compounds Stabilized to Cellular Phosphatases

compd no.	structure	p85 C-SH2 ± SEM[a] (*n*)[b]
2	pTyr-Val-Pro-Met-Leu	0.445 ± 0.047 (16)
8	Ac-pTyr-Val-Pro-Met-NH_2	0.264 ± 0.029 (14)
24	Pmp-Val-Pro-Met-Leu	8.7 (1)
25	CF_2Pmp-Val-Pro-Met-Leu	0.945 ± 0.212 (4)
26	Ac-CF_2Pmp-Val-Pro-Met-NH_2	1.45 ± 0.26 (9)
27	Ac-CF_2Pmp-Val-Ala-N(C_5H_{11})$_2$	0.372 ± 0.053 (8)
28	Ac-CF_2Pmp-Val-Ala-N(C_6H_{13})$_2$	0.446 ± 0.037 (4)

[a] IC_{50} values in micromolar concentrations ± standard error of the mean. [b] *n* = number of determinations.

over src or abl, but compound **16** exhibited a 12-fold selectivity versus src. Similarly, compound **17** was not selective, while compound **18** was 13-fold selective versus src and 65-fold selective versus abl. Interestingly, compounds **20**−**23** were relatively weak inhibitors of both p85 C-SH2 and abl but had enhanced activity versus src.

Analogues Stabilized to Cellular Phosphatases. To evaluate the potential therapeutic utility of this series of phosphorylated peptides, it is critical to demonstrate activity in a whole cell-based model. Unfortunately, it has been shown that phosphorylated tyrosines are rapidly metabolized by intracellular phosphatases.[44] Replacement of phosphotyrosine in compound **2** with the corresponding methylenephosphonate derivative (Pmp, Figure 2, compound **24**) resulted in a 10-fold loss of affinity with respect to compound **2** (Table 2). This loss of affinity has routinely been seen with this substitution in other inhibitors[45−47] and is most likely due to the different pK_{a2} values for the Pmp residue (7.1) versus phosphotyrosine (5.7).[44]

However, it has been reported that the difluorophosphonate derivative (CF_2Pmp, Figure 2) is an acceptable substitution for tyrosine maintaining high-affinity while imparting stability to intracellular phosphatases. In particular, the CF_2Pmp substitution for phosphotyrosine has been successfully incorporated in inhibitors of the src,[36,44,45,48] grb2,[44] and p85[35,46] SH2 domains and inhibitors of the protein tyrosine phosphatases PTP 1 and PTP 1B.[47] In addition, CF_2Pmp has a pK_{a2} value that is much closer to that of phosphotyrosine.[44] Substitution of the CF_2Pmp into the pentapeptide (compound **25** versus **2**) and the tetrapeptide amide (compound **26** versus **8**) resulted in analogues that maintained good affinity. The CF_2Pmp residue was also incorporated into the peptidomimetic dialkylamide series. For compounds **27** and **28**, good affinity versus the parent phosphopeptides (compounds **14** and **18**, respectively) was maintained with IC_{50}'s of 0.372 ± 0.053 μM for the dipentylamide (**27**) and 0.446 ± 0.037 μM for the dihexylamide (**28**). In all cases, the phosphotyrosine-containing peptides were more potent than the corresponding CF_2Pmp analogues.

Since analogues **25** and **26** possessed good affinity for the inhibition of the association of PDGF-β receptor with p85 C-SH2, these compounds were further evaluated in a cellular assay. In this cellular assay, the test compounds were incubated in the presence of rat aortic smooth muscle cells for 5 min. At this point, the medium was treated with rat PDGF-BB (β-homodimer) for an additional 24 h to induce autophosphorylation of the PDGF receptor and association of PI 3-kinase. The medium was removed, the cells were lysed, and the supernatant was incubated with anti-human PDGF-β receptor monoclonal antibody which only recognized the β-isoform of the PDGF receptor. Following electrophoresis, the separated proteins were immunoblotted with anti-rat PI 3-kinase antiserum which recognizes the 85 kDa subunit of PI 3-kinase. Thus, at this point the only PI 3-kinase present must have been associated with the PDGF-β receptor. As can be seen in Figure 3, increasing concentrations of both compounds (**25** and **26**) were able to inhibit the association of PI 3-kinase with PDGF-β receptor in a dose-dependent manner. The IC_{50}'s for these compounds are estimated to be 40 and 38 μM, respectively. Since this is an intracellular event, compounds **25** and **26** must be permeable to the cellular membrane and inhibiting a specific cellular response. This observation is quite remarkable considering the highly charged nature of the molecules.

These compounds were then further evaluated for biological activity in a series of single-cell microinjection assays. These assays allowed the direct evaluation of the intracellular biological consequences of these compounds, as well as providing an opportunity to test their inherent stability in living cells. Thus, the effect of microinjection for compounds **25** and **26** on four distinct insulin-stimulated and PI 3-kinase-dependent biological phenotypes which can be quantitatively evaluated was measured.[49−52] These assays were selected based upon the previous observation that the optimum time for measurement of the four endpoints varied from minutes to hours after microinjection, allowing an assessment of intracellular stability of the injected compounds. Thus, the results of microinjection upon insulin-stimulated membrane ruffling (3 min), *c-fos* expression (60 min), GLUT4 translocation (2 h), and cell cycle progression from G_1 to S phase (14 h) was examined.

Experiments to evaluate the effects of compounds **25** and **26** upon lamellipodia formation (membrane ruffling) are illustrated in Figure 5A,C. Stimulation of the cells with insulin resulted in a rearrangement of the actin network from stress fibers in resting cells to membrane-associated ruffling structures (shown as concentrated areas of rhodamine staining in Figure 5A). Ruffles were found in less than 2% of cells which were not stimulated with insulin and in 94% of stimulated cells (Figure 5C). Microinjection of either compound **25** or compound **26** resulted in the complete inhibition of stress fiber rearrangement. This phenotype was also seen in cells adjacent to cells which were microinjected with either compound, presumably due to membrane permeability (Figure 5, top right).

The effect of each compound was then evaluated upon the expression of the immediate early gene, *c-fos*. Detection of *c-fos* expression by immunofluorescence staining is optimal at 60 min following insulin stimulation.[51] Again, microinjection of either compound **25** or **26** completely inhibited the nuclear detection of *c-fos* expression (Figure 5C). This inhibitory phenotype was also seen in NIH 3T3 cells after stimulation with fibroblast growth factor (FGF; data not shown).

These compounds were also tested for their effect upon insulin-stimulated translocation of the GLUT4 glucose transport protein in 3T3-L1 adipocytes. The movement of the GLUT4 protein from intracellular

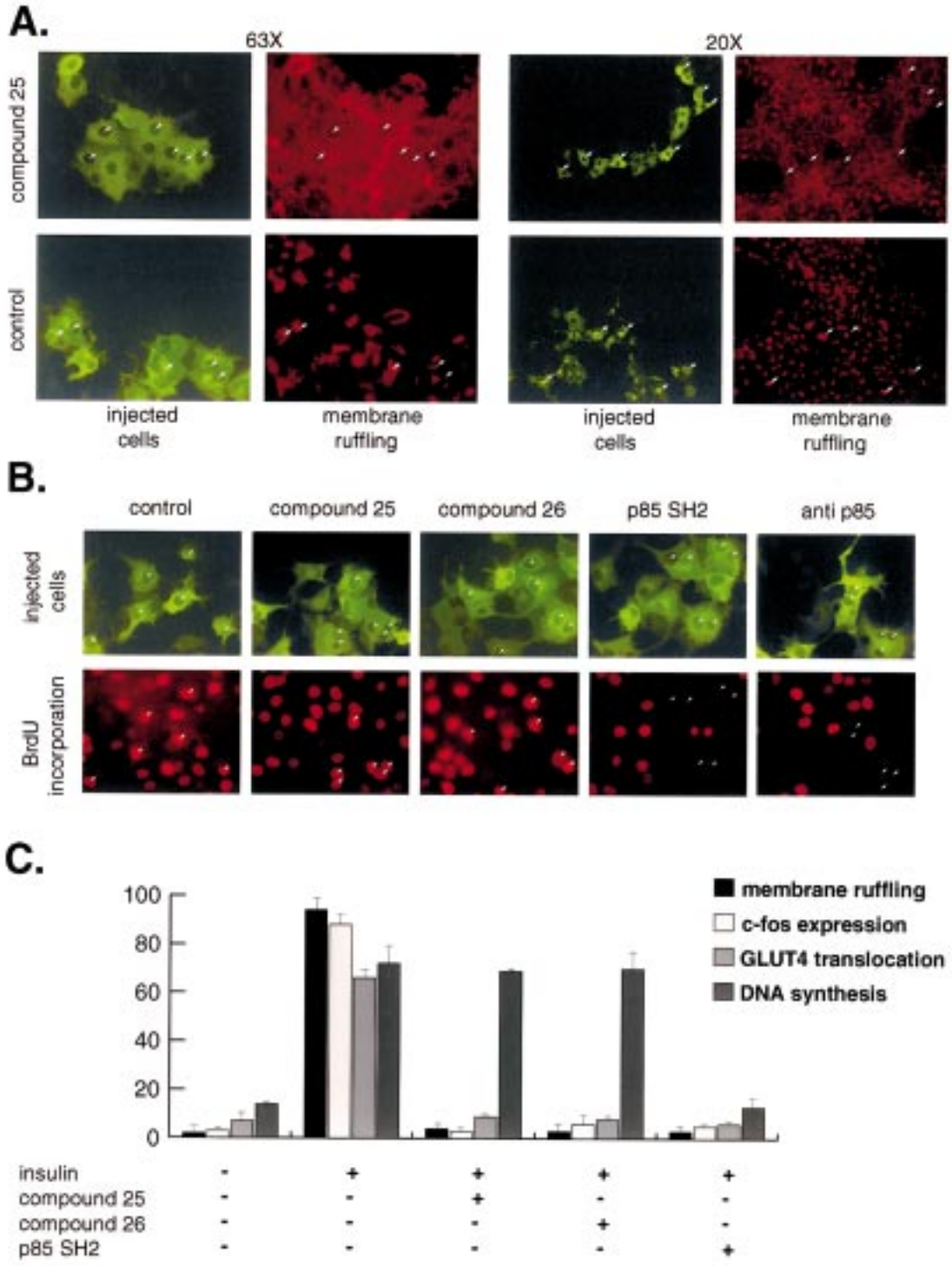

Figure 5. Single-cell microinjection assays. A. Immunofluorescence photomicrographs showing cells injected with compound **25** (top row) or preimmune carrier IgG alone (bottom row). Shown are pictures demonstrating injected cells (green staining) and the same field of cells stained with rhodamine-conjugated phalloidin to show distribution of actin network (red). Arrows are to assist in identification of corresponding cells in each photograph. 63× photographs (left) demonstrate the inhibition of actin rearrangement from stress fibers to membrane-associated lamellipodia following insulin stimulation and injection of compound **25**. 20× photographs (right) demonstrate that this inhibition of membrane ruffling is also detected in adjacent uninjected cells due to the membrane permeability of the compound. B. Photomicrographs showing typical results of DNA synthesis assay. Injected cells possess green fluorescein-stained cytoplasm in contrast to red nuclear staining found in cells which have incorporated BrdU into newly synthesized DNA. Recombinant GST-p85 SH2 domain and anti-p85 IgG are shown as controls. C. Combined results of all four single-cell assays used. Results are expressed as the percentage of cells demonstrating the specific immunofluorescence endpoint ± standard error.

stores in the Golgi apparatus to the plasma membrane as detected by immunofluorescence staining has been used as a single-cell assay for the PI 3-kinase-dependent metabolic effects of insulin in adipocytes.[51,53] The GLUT4 protein is found at the plasma membrane in approximately 5% of cells in the resting state and

translocates in response to physiological insulin concentrations within 2 h in almost 70% of treated cells (Figure 5C). Microinjection of either compound **25** or **26** completely inhibited this insulin-stimulated phenotype.

Finally, both compounds were tested in an assay which requires 14 h of incubation following microinjection to complete. In these experiments, quiescent fibroblasts were injected with each compound, or with GST-p85 SH2 or anti-p85 IgG as controls, and then stimulated with insulin. The cells were labeled with 3-bromo-5′-deoxyuridine (BrdU) to measure progression through G_1 phase of the cell cycle to DNA synthesis. In this case, microinjection of either compound was without any inhibitory effect, despite the complete inhibition seen in cells injected with either of the control proteins. This negative result may be due to the relatively long (14-h) incubation time in these experiments following injection of the compounds. Thus, this lack of inhibition may be a reflection of intracellular instability, but in light of the membrane permeable nature of the compounds it is likely to be a reflection of the loss of concentration in injected cells over the course of the incubation.

The more potent analogues (**27** and **28**) were also evaluated for their ability to block the association of PDGF-β receptor with p85 C-SH2 in rat aortic smooth muscle cells via extracellular administration (as described above). Unfortunately, these compounds resulted in cell detachment and death at the concentrations tested (>25 μM) for reasons that are unknown and were not further investigated. Interestingly, it has been reported that dialkylamides coupled to amino acids possessed good antimicrobial activities but did not induce hemolysis of red blood cells (i.e., were not cytotoxic against a eucaryotic cell line).[54] In addition, it has been reported that peptides rich in α,α-dialkylated amino acids display potent antibacterial activity.[55] Perhaps, the cytotoxicity of compounds **27** and **28** is related to the highly hydrophobic nature of these molecules.

Conclusions

A phosphorylated pentapeptide (pTyr-Val-Pro-Met-Leu, compound **2**) from the kinase insert region of PDGF-β receptor inhibits the complexation of PDGF β-receptor with the C-terminal SH2 domain of PI 3-kinase with an IC_{50} of 0.445 ± 0.04μM. Structural modifications via classical medicinal chemistry approaches resulted in a tetrapeptide (Ac-pTyr-Val-Pro-Met-NH_2, compound **8**) with enhanced activity (IC_{50} = 0.264 ± 0.029 μM). Dialkylamides substituted for the C-terminal methionine residue were shown to enhance affinity. In fact, the dihexylamide represents the most potent analogue reported to date with an IC_{50} of 0.076 ± 0.010 μM (compound **18**). In addition, compound **18** was shown to possess good selectivity for p85 C-SH2 over src and abl SH2 domains. Analogues stabilized against intracellular phosphatases were also prepared by the incorporation of the CF_2Pmp moiety for pTyr (compounds **25** and **26**). These compounds maintained good affinity with IC_{50}'s of 0.945 ± 0.212 and 1.45 ± 0.26 μM for p85 C-SH2, respectively. Compounds **25** and **26** were able to block the association of PDGF-β receptor with the C-terminal SH2 domain of p85 PI 3-kinase when administered extracellularly to rat aortic smooth muscle cells with IC_{50}'s of 40 and 38 μM, respectively. In addition, these compounds were shown to have specific cellular effects upon microinjection. The potency of these analogues was further enhanced in the dialkylamide series. For example, compounds **27** and **28** possessed IC_{50}'s of 0.372 ± 0.053 and 0.446 ± 0.037 μM, respectively, but unfortunately these compounds proved to be cytotoxic in the whole cell assay.

The concerns raised in our introduction regarding the utility of peptides/phosphopeptides and/or phosphopeptidomimetics for the treatment of restenosis can, at least in part, be addressed via design of the appropriate analogue. In particular, the N-terminal acetylation and C-terminal amidation impart stability to exopeptidases. The CF_2Pmp substitution for pTyr incorporates stability to intracellular phosphatases while maintaining good affinity. In addition, results from the whole cellular experiments with compounds **25** and **26** demonstrate that a specific intracellular event can be modulated via extracellular administration of a therapeutic agent even if highly charged. However, the concern of drug delivery has yet to be addressed. It is envisioned that the resulting drug could be delivered directly to the point of injury (i.e., lesion resulting from PTCA) via the catheter during the balloon angioplasty procedure.

Experimental Section

Materials and Methods. The orthogonally protected N^{α}-*t*-Boc and N^{α}-Fmoc amino acids and the resins Wang (HMP, *p*-benzyloxybenzyl alcohol),[56] Rink amide,[38,39] and Sasrin[40,41] were purchased from either Bachem Bioscience, Advanced Chemtech, or Peninsula Laboratories, Inc. The unnatural amino acids N^{α}-Fmoc-diethyl-4-phosphonomethylphenylalanine [N^{α}-Fmoc-Pmp$(OEt)_2$] and N^{α}-*t*-Boc-diethyl-4-phosphono-(difluoromethyl)phenylalanine [N^{α}-*t*-Boc-CF_2Pmp$(OEt)_2$] were prepared by previously reported methods.[57] All amino acids were of the L-configuration unless otherwise indicated.

Trifluoroacetic acid (TFA) was purchased from Halocarbon. *N,N′*-Dicyclohexylcarbodiimide (DCC), diisopropylethylamine (DIEA), and HOBt were purchased from Applied Biosystems Inc. (ABI). *N,N*-Dimethylformamide (DMF), dichloromethane (DCM), *N*-methylpyrrolidone (NMP), and methanol (MeOH) were purchased from Burdick & Jackson (reagent grade or better). Acetonitrile (AcCN) and water (HPLC grade) were purchased from Mallinckrondt and EM Science, respectively. Trimethylsilyl trifluoromethanesulfonate (TMSOTf), dimethyl sulfide (DMS), ethanedithiol (EDT), phenol, thioanisole, *m*-cresol, bromoacetic acid, diisopropylcarbodiimide (DIC), 1*H*-tetrazole, di-*tert*-butyl diethylphosphoramidite, *N*-methylmorpholine (NMM), 1-(3-dimethylaminopropyl)-3-ethylcarbodiimide hydrochloride (EDCI), and *tert*-butyl hydroperoxide were purchased from Aldrich Chemical Co., Inc. *O*-(7-Azabenzotriazol-1-yl)-1,1,3,3-tetramethyluronium hexafluorophosphate (HATU) and 1*H*-hydroxy-7-azabenzotriazole (HOAt) were purchased from PerSeptive Biosystems.

The peptides were prepared on an ABI model 431A automated peptide synthesizer using software version 1.00 for Fmoc synthesis. RP-HPLC was performed on a Waters HPLC system from Millipore Corp. equipped with a model 600E system controller, a model 600 solvent delivery system, a model 490 variable wavelength detector at 214 and 280 nm, and a model 717 plus autosampler. Vydac analytical and preparative C18 RP-HPLC columns were purchased from Resolution Systems. Preparative RP-HPLC was performed using a C18 preparative scale Vydac column (218TP1022, 2.2 × 25.0 cm, 10−20-μm particle size) eluting with a linear gradient of 0.1% aqueous TFA with increasing concentrations of AcCN at 15 mL/min. Analytical RP-HPLC analyses were performed on a

Vydac column (218TP54, 0.46 × 25.0 cm, 5-μm particle size). The conditions for analytical RP-HPLC were as follows: 100:0 to 34:66 0.1% aqueous TFA−0.1% TFA in AcCN, linear gradient over 22 min at 1.5 mL/min (λ = 214 and 280 nm).

Electrospray mass spectra (ESMS) were determined with a Fisons VG Trio 2000 quadrupole mass spectrometer using a 1.0% 50:50 water−methanol in acetic acid solution. Fast atom bombardment mass spectra (FABMS) were obtained on a VG analytical 7070E/HF mass spectrometer in a matrix of either thioglycerol or 3-nitrobenzyl alcohol using xenon as the target gas.

Synthetic Chemistry. Method A: The peptides (compounds **1**−**10**) were synthesized by solid-phase peptide synthetic techniques on an ABI 431A automated peptide synthesizer on a 0.25-mmol scale. The C-terminal carboxylates were prepared on a Wang resin,[56] while the C-terminal carboxamides were assembled on a Rink amide[38,39] resin using an N^{α}-Fmoc protection strategy.[58,59] Individual N^{α}-Fmoc amino acids were coupled as their preformed symmetrical anhydrides with DCC in NMP. At each step the N^{α}-Fmoc group was removed with 20% piperidine in NMP. Acetylation of the N-terminus was performed on the resin with 50% acetic anhydride in DCM. The peptides were cleaved from the resin using TFA−water−phenol−thioanisole−ethanedithiol (82.5:5.0:5.0:5.0:2.5).[60] The crude peptides were then solubilized in AcCN/water and lyophilized. The resulting crude peptide was purified by RP-HPLC.

Method B: For the peptidomimetic tripeptides (compounds **11**−**16**), the tripeptide Ac-Tyr(Bzl)-Val-Ala was prepared on a Sasrin resin[40,41] (5.0 mmol of free alcohol total) in a manual shaker employing the same solid-phase peptide synthesis techniques as above. After resin cleavage with 1% TFA in DCM and lyophilization the appropriate amine (5.0 equiv) was coupled using EDCI (5 equiv), HOBt (5.0 equiv), and NMM (5.0 equiv) in tetrahydrofuran (THF; 6 h). Debenzylation of tyrosine was achieved with hydrogen under pressure (50−55 psi) with 20% Pd/C in methanol. The tripeptides were then phosphitylated with 2.63 g (37.5 mmol) of 1*H*-tetrazole and 3.12 g (12.5 mmol) of di-*tert*-butyl diethylphosphoramidite.[61] The peptide resin was then oxidized with 0.68 mL (5.0 mmol) of 70% aqueous *tert*-butyl hydroperoxide. The compounds were cleaved with 95% TFA/5% water, concentrated under reduced pressure, resuspended in water (∼100 mL), and lyophilized. The resulting crude diastereomeric peptidomimetics were purified and separated by RP-HPLC.

Method C: For the peptidomimetic tripeptides (compounds **17**−**23**), the tripeptide Ac-Tyr(Bzl)-Val-Ala or Ac-Tyr(Bzl)-Val-D-Ala was prepared on a Sasrin resin[40,41] (5.0 mmol of free alcohol total) in a manual shaker employing the same solid-phase peptide synthesis techniques as above on a 5.0-mmol scale. After resin cleavage with 1% TFA in DCM and lyophilization, the appropriate amine (5.0 equiv) was coupled using HATU (5.0 equiv), HOAt (5.0 equiv), and NMM (5.0 equiv) in THF (6 h). Debenzylation of tyrosine was achieved with hydrogen under pressure (50−55 psi) with 20% Pd/C in methanol. The tripeptides were then phosphitylated with 2.63 g (37.5 mmol) of 1*H*-tetrazole and 3.12 g (12.5 mmol) of di-*tert*-butyl diethylphosphoramidite.[61] The compound was then oxidized with 0.68 mL (5.0 mmol) of 70% aqueous *tert*-butyl hydroperoxide. The compounds were cleaved with 95% TFA/5% water, concentrated under reduced pressure, resuspended in water (∼100 mL), and lyophilized. The resulting crude diastereomeric peptidomimetics were purified and separated by RP-HPLC.

Method D: The peptides (compounds **24**−**26**) were synthesized as in method A with the exception that TFA−TMSOTf−DMS−EDT−*m*-cresol (65:19:15:0.8:0.2) was utilized for the resin cleavage and deprotection.[62]

Method E: The peptidomimetic tripeptides (compounds **27** and **28**) were synthesized as in method C with the exception that TFA−TMSOTf−DMS−EDT−*m*-cresol (65:19:15:0.8:0.2) was utilized for the resin cleavage and deprotection.

Peptide Purification. The crude peptides/peptidomimetics were dissolved in a mixture of aqueous 0.1% TFA and AcCN and then purified by preparative RP-HPLC as described above. Fractions determined to be pure by analytical RP-HPLC were combined, concentrated under reduced pressure, and lyophilized.

Peptide Purity and Characterization. The purified peptides/peptidomimetics were assessed for purity by analytical RP-HPLC and characterized by ESMS or FABMS.

Preparation of pTyr-Met-Asp-Met-Ser (1). The peptide synthesis, cleavage of the resin, and deprotection were performed as described in the aforementioned general procedure (method A) to afford 35 mg of the title compound: HPLC t_R = 10.0 min (>99%); FABMS $(m/z)^+$ calcd 725.74, found 726.2 (M + 1).

Preparation of pTyr-Val-Pro-Met-Leu (2). The peptide synthesis, cleavage of the resin, and deprotection were performed as described in the aforementioned general procedure (method A) to afford 87 mg of the title compound: HPLC t_R = 14.0 min (>99%); ESMS $(m/z)^+$ calcd 701.78, found 702.2 (M).

Preparation of pTyr-Val-Pro-Met (3). The peptide synthesis, cleavage of the resin, and deprotection were performed as described in the aforementioned general procedure (method A) to afford 6 mg of the title compound: HPLC t_R = 13.2 min (>99%); ESMS $(m/z)^+$ calcd 588.20, found 590.0 (M).

Preparation of Ac-pTyr-Val-Pro-Met-Leu (4). The peptide synthesis, cleavage of the resin, and deprotection were performed as described in the aforementioned general procedure (method A) to afford 37 mg of the title compound: HPLC t_R = 17.7 min (>98%); ESMS $(m/z)^+$ calcd 743.82, found 744.0 (M).

Preparation of pTyr-Val-Pro-Met-Leu-NH_2 (5). The peptide synthesis, cleavage of the resin, and deprotection were performed as described in the aforementioned general procedure (method A) to afford 99 mg of the title compound: HPLC t_R = 15.8 min (>98%); ESMS $(m/z)^+$ calcd 700.80, found 700.5 (M).

Preparation of Ac-pTyr-Val-Pro-Met-Leu-NH_2 (6). The peptide synthesis, cleavage of the resin, and deprotection were performed as described in the aforementioned general procedure (method A) to afford 18 mg of the title compound: HPLC t_R = 17.1 min (>98%); ESMS $(m/z)^+$ calcd 742.86, found 742.4 (M).

Preparation of pTyr-Val-Pro-Met-NH_2 (7). The peptide synthesis, cleavage of the resin, and deprotection were performed as described in the aforementioned general procedure (method A) to afford 43 mg of the title compound: HPLC t_R = 10.4 min (>99%); ESMS $(m/z)^+$ calcd 587.64, found 589.1 (M).

Preparation of Ac-pTyr-Val-Pro-Met-NH_2 (8). The peptide synthesis, cleavage of the resin, and deprotection were performed as described in the aforementioned general procedure (method A) to afford 35 mg of the title compound: HPLC t_R = 11.5 min (>99%); ESMS $(m/z)^+$ calcd 629.64, found 630.3 (M).

Preparation of pTyr-Val-Pro-Nle-NH_2 (9). The peptide synthesis, cleavage of the resin, and deprotection were performed as described in the aforementioned general procedure (method A) to afford 8 mg of the title compound: HPLC t_R = 18.6 min (>97%); ESMS $(m/z)^+$ calcd 683.75, found 684.6 (M).

Preparation of Ac-pTyr-Val-Ala-*N*-BuGly-NH_2 (10). Initially, 0.42 g (3.0 mmol) of bromoacetic acid was coupled to a Rink amide[38,39] resin (0.25 mmol of free amine total) with 0.52 mL (3.3 mmol) of diisopropylcarbodiimide for 30 min in a manual shaker,[37] the resin was washed with DMSO (2×), and *N*-butylamine (0.99 mL, 10.0 mmol) was added and allowed to mix for 2.5 h. The remaining peptide synthesis, cleavage of the resin, and deprotection were performed as described in the aforementioned general procedure (method A) to afford 34 mg of the title compound: HPLC t_R = 11.9 min (>99%); ESMS $(m/z)^-$ calcd 585.60, found 584.5 (M).

Preparation of Ac-pTyr-Val-Ala-NHC_5H_{11} (11). The peptide synthesis, cleavage of the resin, and deprotection were performed as described in the aforementioned general procedure (method B) to afford 4 mg of the title compound: HPLC t_R = 13.6 min (>99%); ESMS $(m/z)^-$ calcd 542.57, found 541.4 (M).

Preparation of Ac-pTyr-Val-D-Ala-NHC$_5$H$_{11}$ (12). The peptide synthesis, cleavage of the resin, and deprotection were performed as described in the aforementioned general procedure (method B) to afford 2 mg of the title compound: HPLC t_R = 14.0 min (>99%); ESMS (m/z)$^-$ calcd 542.57, found 541.4 (M).

Preparation of Ac-pTyr-Val-D-Ala-N(C$_5$H$_{11}$)$_2$ (13). The peptide synthesis, cleavage of the resin, and deprotection were performed as described in the aforementioned general procedure (method B) to afford 17 mg of the title compound: HPLC t_R = 13.4 min (>99%); ESMS (m/z)$^-$ calcd 612.71, found 611.5 (M).

Preparation of Ac-pTyr-Val-Ala-N(C$_5$H$_{11}$)$_2$ (14). The peptide synthesis, cleavage of the resin, and deprotection were performed as described in the aforementioned general procedure (method B) to afford 6 mg of the title compound: HPLC t_R = 13.1 min (>96%); ESMS (m/z)$^-$ calcd 612.71, found 611.6 (M).

Preparation of Ac-pTyr-Val-D-Ala-N(C$_4$H$_9$)$_2$ (15). The peptide synthesis, cleavage of the resin, and deprotection were performed as described in the aforementioned general procedure (method B) to afford 22 mg of the title compound: HPLC t_R = 10.7 min (>97%); ESMS (m/z)$^-$ calcd 584.66, found 583.6 (M).

Preparation of Ac-pTyr-Val-Ala-N(C$_4$H$_9$)$_2$ (16). The peptide synthesis, cleavage of the resin, and deprotection were performed as described in the aforementioned general procedure (method B) to afford 17 mg of the title compound: HPLC t_R = 10.3 min (>93%); ESMS (m/z)$^-$ calcd 584.66, found 583.6 (M).

Preparation of Ac-pTyr-Val-D-Ala-N(C$_6$H$_{13}$)$_2$ (17). The peptide synthesis, cleavage of the resin, and deprotection were performed as described in the aforementioned general procedure (methods B and C) to afford 32 mg of the title compound via method C: HPLC t_R = 15.8 min (>99%); ESMS (m/z)$^-$ calcd 640.76, found 639.6 (M).

Preparation of Ac-pTyr-Val-Ala-N(C$_6$H$_{13}$)$_2$ (18). The peptide synthesis, cleavage of the resin, and deprotection were performed as described in the aforementioned general procedure (methods B and C) to afford 11 mg of the title compound via method C: HPLC t_R = 15.7 min (>99%); ESMS (m/z)$^-$ calcd 640.76, found 639.3 (M).

Preparation of Ac-pTyr-Val-Ala-N(C$_8$H$_{17}$)$_2$ (19). The peptide synthesis, cleavage of the resin, and deprotection were performed as described in the aforementioned general procedure (method C) to afford 68 mg of the title compound: HPLC t_R = 15.5 min (>99%); ESMS (m/z)$^-$ calcd 696.87, found 696.4 (M).

Preparation of Ac-pTyr-Val-D-Ala-NH(CH$_2$)$_2$-C$_6$H$_5$ (20). The peptide synthesis, cleavage of the resin, and deprotection were performed as described in the aforementioned general procedure (method C) to afford 21 mg of the title compound: HPLC t_R = 10.7 min (>99%); ESMS (m/z)$^-$ calcd 576.59, found 575.5 (M).

Preparation of Ac-pTyr-Val-Ala-NH(CH$_2$)$_2$-C$_6$H$_5$ (21). The peptide synthesis, cleavage of the resin, and deprotection were performed as described in the aforementioned general procedure (method C) to afford 23 mg of the title compound: HPLC t_R = 14.2 min (>99%); ESMS (m/z)$^-$ calcd 576.59, found 575.3 (M).

Preparation of Ac-pTyr-Val-D-Ala-NH(CH$_2$)$_2$-C$_6$H$_{11}$ (22). The peptide synthesis, cleavage of the resin, and deprotection were performed as described in the aforementioned general procedure (method C) to afford 12 mg of the title compound: HPLC t_R = 9.4 min (>99%); ESMS (m/z)$^-$ calcd 582.64, found 581.6 (M).

Preparation of Ac-pTyr-Val-Ala-NH(CH$_2$)$_2$-C$_6$H$_{11}$ (23). The peptide synthesis, cleavage of the resin, and deprotection were performed as described in the aforementioned general procedure (method C) to afford 9 mg of the title compound: HPLC t_R = 9.8 min (>99%); ESMS (m/z)$^-$ calcd 582.64, found 581.4 (M).

Preparation of Pmp-Val-Pro-Met-Leu (24). The peptide synthesis, cleavage of the resin, and deprotection were performed as described in the aforementioned general procedure (method D) to afford 9 mg of the title compound: HPLC t_R = 17.6 min (>98%); ESMS (m/z)$^-$ calcd 699.81, found 699.3 (M).

Preparation of CF$_2$Pmp-Val-Pro-Met-Leu (25). The peptide synthesis, cleavage of the resin, and deprotection were performed as described in the aforementioned general procedure (method D) to afford 57 mg of the title compound: HPLC t_R = 14.2 min (>99%); ESMS (m/z)$^-$ calcd 735.79, found 735.3 (M).

Preparation of CF$_2$Pmp-Val-Pro-Met-NH$_2$ (26). The peptide synthesis, cleavage of the resin, and deprotection were performed as described in the aforementioned general procedure (method D) to afford 44 mg of the title compound: HPLC t_R = 11.0 min (>99%); ESMS (m/z)$^-$ calcd 622.65, found 622.3 (M).

Preparation of Ac-CF$_2$Pmp-Val-Ala-N(C$_5$H$_{11}$)$_2$ (27). The peptide synthesis, cleavage of the resin, and deprotection were performed as described in the aforementioned general procedure (method E) to afford 5 mg of the title compound: HPLC t_R = 16.4 min (>99%); ESMS (m/z)$^-$ calcd 646.72, found 645.4 (M).

Preparation of Ac-CF$_2$Pmp-Val-Ala-N(C$_6$H$_{13}$)$_2$ (28). The peptide synthesis, cleavage of the resin, and deprotection were performed as described in the aforementioned general procedure (method E) to afford 16 mg of the title compound: HPLC t_R = 19.9 min (>85%); ESMS (m/z)$^-$ calcd 674.77, found 673.6 (M).

Molecular Modeling. The homology modeling was performed using SYBYL software package (version 6.0)[63] and a Silicon Graphics workstation. Due to the overall similarity of the sequences and loop sizes of syp N-terminal SH2 domain and p85 C-SH2, the 2.05 Å X-ray structure of syp N-terminal SH2 domain bound to the high-affinity PDGF receptor sequence of Val-Leu-pTyr-Thr-Ala-Val-Gln-Pro[64] was used as a basis coordinate set in designing a three-dimensional homology model of p85 C-SH2. The sequence alignment used was that published by Lee et al.[64] Subsequently, the NMR structures of p85 N-SH2[65] and PLCγ-SH2 domains[66] were used to model short portions of the p85 C-SH2 sequence that showed greater local similarity. (Note: at the time that this work was performed, the NMR structure of p85 SH2 had not been reported.[33]) The starting model for the parent molecule (compound **2**) was based upon the structure of the high-affinity PDGF receptor sequence of Val-Leu-pTyr-Thr-Ala-Val-Gln-Pro starting from residue 740 bound to syp N-terminal SH2 domain[64] and was modified to the various peptide structures which were each manually docked into the p85 C-SH2 domain model and minimized. In particular, the aliphatic groups at the p + 3 site were modeled (1) into the pY + 3 pocket based on the +3 Val conformation in the syp-bound PDGF sequence and (2) into the nearby hydrophobic channel based on the conformation of the +3/+4 PDGF backbone sequence. Minimizations of the inhibitor models and protein model were carried out using the Tripos force field.[63]

Expression and Purification of the C-Terminal SH2 Domain of the p85 Subunit of PI 3-Kinase−GST Fusion Protein (GST p85 C-SH2). The pGEX plasmid expressing the GST p85 C-SH2 fusion protein was used in these studies. Both the expression and purification of the fusion protein were performed as previously described.[67] To prepare the [^{35}S]GST p85 C-SH2 fusion protein, a 75-mL overnight culture of *Escherichia coli* expressing the GST p85 fusion protein was added to 1.0 L of LB broth containing 100 μg/mL ampicillin. The cultures were incubated at 37 °C until reaching a density of A_{600} = 1.0. Isopropyl thio-β-D-galactoside (1 mM) was added; 15 min later, 10 mCi of *trans*-^{35}S-label was added and cultures were incubated for an additional 3 h at 37 °C. The cells were then lysed by sonication and fusion proteins purified by affinity chromatography using glutathione-agarose (CL-4B) beads.

Preparation of the Intracellular Tyrosine Kinase Domain of the PDGF-β Receptor. Lysates from SF9 insect cells expressing the PDGF-β receptor tyrosine kinase (PDGFR-TK) were incubated with M2 affinity beads, and the complexes were washed several times with Tris buffer containing pro-

tease inhibitors and sodium orthovanadate. Complexes were centrifuged and resuspended in HEPES buffer containing 1 mM ATP, 10 mM $MnCl_2$, and 5 mM $MgCl_2$ to stimulate phosphorylation of the PDGFR-TK.

GST p85 C-SH2−PDGFR-TK Binding Assay. Binding of [^{35}S]GST p85 C-SH2 fusion proteins to the phosphorylated PDGFR-TK was assayed in 20 mM HEPES buffer containing 10 μg/mL each of the protease inhibitors, phenylmethanesulfonyl fluoride (PMSF), pepstatin, leupeptin, and aprotinin with 0.5 mM EDTA and 0.1% NP-40. The binding assays were performed in 96-well Millipore filter plates in a final volume of 250 μL of HEPES buffer containing 135 μL of phosphorylated PDGFR-TK beads complex (1 μg of receptor/well), 10 μL of [^{35}S]GST p85 C-SH2 fusion protein (30 000 cpm/well), and 5 μL of peptide inhibitor as indicated. Samples were incubated at 25 °C for 20 min with continuous rocking. Binding was terminated by filtration through the filter plates using a Millipore multiscreen filtration manifold. Filter plates were washed four times with 150 μL of HEPES buffer followed by the addition of 30 μL of Hi-load scintillant. The radioactivity that was retained on the filters was counted in a Wallac 1450 Microbeta counter. Total binding was defined as [^{35}S]GST p85 C-SH2 fusion protein bound to the PDGFR-TK bead complex retained on the filter plates. Specific binding was defined as total binding minus nonspecific binding. IC_{50} values were calculated by weighted nonlinear regression curve fitting.

GST−src and −abl SH2 Domain Binding Assays. These assays were performed as previously described.[21,22]

PDGF Receptor/PI 3-Kinase Cell Association Assay. Rat aortic smooth muscle cells were grown to confluency in 100-mm dishes. Growth medium was removed and replaced with serum-free medium, and cells were incubated at 37 °C for an additional 24 h. Test compounds were then added directly to the medium and cells incubated for an additional 24 h. At this point, rat PDGF-BB (β-homodimer) was added at a final concentration of 30 ng/mL for 5 min at 37 °C to stimulate autophosphorylation of the PDGF-β receptor and association of PI 3-kinase to the phosphorylated receptors. Following growth factor treatment, the medium was removed, and cells were washed with cold phosphate-buffered saline and immediately lysed with 1 mL of lysis buffer [50 mM HEPES (pH 7.5), 150 mM NaCl, 10% glycerol, 1.0% Triton-X 100, 1 mM EDTA, 1 mM EGTA, 50 mM NaF, 1 mM sodium orthovanadate, 30 mM *p*-nitrophenyl phosphate, 10 mM sodium pyrophosphate, 1 mM PMSF, 10 μg/mL aprotinin, and 10 μg/mL leupeptin]. Lysates were centrifuged at 10000*g* for 10 min. Supernatants were incubated for 2 h with 10 μL of anti-human PDGF receptor polyclonal antibody (1:1000) which recognizes the PDGF receptor β-isoform. Following the incubation, protein-A-sepharose beads were added for 2 h with continuous mixing and immune complexes bound to the beads washed four times with 1 mL of lysis wash buffer. Immune complexes were solubilized in 30 μL of Laemmli sample buffer and electrophoresed in 4−20% SDS−polyacrylamide gels. Following electrophoresis, separated proteins were transferred to nitrocellulose and immunoblotted with anti-rat PI 3-kinase antiserum which recognizes the 85-kDa subunit of PI 3-kinase. Following incubation with [^{125}I]protein-A, p85 protein levels were detected by phosphorimage analysis and protein bands quantitated via densitometry. IC_{50} values were generated from the densitometric data.

Microinjection Experiments. The procedures used for the microinjection of purified antibodies and fusion proteins has been previously described.[49] Insulin-responsive rat 1 fibroblasts were maintained[68] and stimulated where indicated with 100 ng/mL insulin. 3T3-L1 adipocytes were cultured and differentiated using established methods and injected.[53] Cells were plated on 12-mm glass coverslips and were rendered quiescent by incubation in serum-free medium for 24−36 h. Cells were microinjected with either compound **25** or **26** (50 μM), recombinant GST−p85 SH2 domain fusion protein (12 mg/mL), or a polyclonal affinity-purified anti-p85 IgG (3.5 mg/mL) (a gift from Lou Cantley). Preimmune IgG of the appropriate species was added to all samples to give a final concentration of 5 mg/mL to allow the unambiguous identification of microinjected cells. Each experiment was conducted a minimum of three separate times, with at least 250 cells injected on each occasion. After injection, cells were stimulated and stained for immunofluorescence microscopy as described below. Results were analyzed on a Zeiss Axiophot epifluorescence microscope, and digital photography was accomplished with a Photometrix CCD camera.

Single-Cell Immunofluorescence Assays. 1. DNA Synthesis. Two hours following injection, BrdU was added to the medium, and the cells were incubated at 37 °C for 16 h.[69] Cells were then fixed in 3.7% formaldehyde and stained with a monoclonal anti-BrdU antibody (Accurate Scientific). Incorporation of BrdU into newly synthesized DNA (an indication of progression of the cells into S phase) was detected by simultaneous staining with rhodamine anti-rat IgG and fluorescein anti-rabbit IgG.[70] This staining method results in red nuclear staining in cells which have incorporated BrdU and green cytoplasmic staining in cells which were microinjected.

2. GLUT4 Translocation. One hour after injection, differentiated 3T3-L1 cells were treated with or without 10 ng/mL insulin for 2 h and then fixed, permeabilized, and stained[50] using affinity-purified rabbit polyclonal antibody F349 (a gift from Mike Mueckler) raised against GLUT4. Detection of GLUT4 distribution in the cells was detected with fluorescein anti-rabbit IgG, and injected cells were identified by staining with rhodamine anti-sheep IgG. This single-cell assay for insulin-stimulated glucose uptake was then quantitated by assessment of the translocation of the GLUT4 transporter from its intracellular stores in the trans Golgi apparatus to the plasma membrane.[53]

3. *c-fos* Expression. One hour after injection, cells were stimulated with 100 ng/mL insulin where indicated and fixed in 3.7% formaldehyde after 60 min of stimulation.[51] Nuclear *c-fos* expression was detected in single cells by staining with polyclonal anti-fos-specific rabbit IgG (Oncogene Science),[51] followed by rhodamine anti-rabbit IgG and fluorescein anti-sheep IgG to detect injected cells. Results were quantitated by assessment of nuclear rhodamine staining.

4. Membrane Ruffling. Thirty minutes after injection, cells were stimulated with 100 ng/mL insulin where indicated for 3 min and then fixed and stained.[52] Ruffling was detected by staining with rhodamine-conjugated phalloidin, and injected cells were detected with fluorescein anti-rabbit IgG. Lamellipodia (membrane ruffles) were quantitated by visualization of actin rearrangement from organized stress fibers in unstimulated cells to concentrated areas of actin-containing ruffles at the plasma membrane.

Acknowledgment. The authors wish to thank Darin R. Kent for the preparation of compound **19**. The authors also thank James H. Fergus and Susan Hubbell for providing the selectivity data.

References

(1) Lechleider, R. J.; Sugimoto, S.; Bennett, A. M.; Kashishian, A. S.; Cooper, J. A.; Shoelson, S. E.; Walsh, C. T.; Neel, B. G. Activation of the SH2-containing phosphotyrosine phosphatase SH-PTP2 by its binding site, phosphotyrosine 1009, on the human platelet-derived growth factor receptor β. *J. Biol. Chem.* **1993**, *268*, 21478−21481.

(2) Fry, M. J.; Panayotou, G.; Booker, G. W.; Waterfield, M. D. New insights into protein-tyrosine kinase receptor signaling complexes. *Protein Sci.* **1993**, *2*, 1785−1797.

(3) Beattie, J. SH2 domain protein interaction and possibilities for pharmacological intervention. *Cell. Signal.* **1996**, *8*, 75−86.

(4) Capron, L.; Heudes, D.; Chajara A.; Bruneval, P. Effect of ramipril, an inhibitor of angiotensin converting enzyme, on the response of rat thoracic aorta to injury with a balloon catheter. *J. Cardiovasc. Pharmacol.* **1991**, *18*, 207−211.

(5) Bourassa, M. Silent myocardial ischemia after coronary angioplasty: distinguishing the shadow from the substance. *J. Am. Coll. Cardiol.* **1992**, *19*, 1410−1411.

(6) Herrman, J. R.; Hermans, W. R. M.; Vos, J.; Serruys, P. W. Pharmacological approaches to the prevention of restenosis following angioplasty. *Drugs* **1993**, *46*, 18−52.

(7) Gordon, D.; Reidy, M. A.; Benditt, E. P.; Schwartz, S. M. Cell proliferation in human coronary arteries. *Proc. Natl. Acad. Sci. U.S.A.* **1990**, *87*, 4600−4604.

(8) Majesky, M. W.; Reidy, M. A.; Bowen-Pope, D. F.; Hart, C. E.; Wilcox, J. N.; Schwartz, S. M.; PDGF ligand and receptor gene expression during repair of arterial injury. *J. Cell Biol.* **1990**, *111*, 2149−2158.

(9) Jawien, A.; Bowen-Pope, D. F.; Lindner, V.; Schwartz, S. M.; Clowes, A. W. Platelet-derived growth factor promotes smooth muscle migration and initimal thickening in a rat model of balloon angioplasty. *J. Clin. Invest.* **1992**, *89*, 507−511.

(10) Ferns, G. A. A.; Raines, E. W.; Sprugel, K. H.; Motani, A. S.; Reidy, M. A.; Ross, R. Inhibition of neointimal smooth muscle accumulation after angioplasty by an antibody to PDGF. *Science* **1991**, *253*, 1129−1132.

(11) Birge, R. B.; Hanafusa, H. Closing in on SH2 specificity. *Science* **1993**, 262, 1522−1524.

(12) Pawson, T. Protein modules and signaling networks. *Nature* **1995**, *373*, 573−580.

(13) Marengere, L. E. M.; Pawson, T. Structure and function of SH2 domains. *J. Cell Sci.* **1994**, *18*, 97−104.

(14) Fantl, W. J.; Escobedo, J. A.; Martin, G. A.; Turck, C. W.; del Rosario, M.; McCormick, F.; Williams, L. T. Distinct phosphotyrosines on a growth factor receptor bind to specific molecules that mediate different signaling pathways. *Cell* **1992**, *69*, 413−423.

(15) Kaplan, D. R.; Morrison, D. K.; Wong, G.; McCormick, F.; Williams, L. T. PDGF β-receptor stimulates tyrosine phosphorylation of GAP and association of GAP with a signaling complex. *Cell* **1990**, *61*, 125−133.

(16) Koch, A.; Anderson, D.; Moran, M.; Ellis, C.; Pawson, T. SH2 and SH3 domains: elements that control interactions of cytoplasmic signaling proteins. *Science* **1991**, *252*, 668−674.

(17) Panayotou, G.; Gish, G.; End, P.; Troung, O.; Gout, I.; Dhand, R.; Fry, M. J.; Hiles, I.; Pawson, T.; Waterfield, M. D. Interactions between SH2 domains and tyrosine-phosphorylated platelet-derived growth factor β-receptor sequences: Analysis of kinetic parameters by a novel biosensor-based approach. *Mol. Cell. Biol.* **1993**, *13*, 3567−3576.

(18) Klippel, A.; Escobedo, J. A.; Fantl, W. J.; Williams, L. T. The C-terminal SH2 domain of p85 accounts for the high affinity and specificity of the binding of phosphatidylinositol 3-kinase to phosphorylated platelet-derived growth factor β receptor. *Mol. Cell. Biol.* **1992**, *12*, 1451−1459.

(19) Songyang, Z.; Shoelson, S. E.; Chaudhuri, M.; Gish, G.; Pawson, T.; Haser, W. G.; King, F.; Roberts, T.; Ratnofsky, S.; Lechleider, R. J.; Neel, B. G.; Birge, R. B.; Fajardo, J. E.; Chou, M. M.; Hanafusa, H.; Schaffhausen, Cantley, L. C. SH2 domains recognize specific phosphopeptide sequences. *Cell* **1993**, *72*, 767−778.

(20) Cantley, L. C.; Songyang, Z. Specificity in recognition of phosphopeptides by src-homology 2 domains. *J. Cell Sci.* **1994**, *18*, 121−126.

(21) Plummer, M. S.; Lunney, E. A.; Para, K. S.; Shahripour, A.; Stankovic, C. J.; Humblet, C.; Fergus, J. H.; Marks, J. S.; Herrera, R.; Hubbell, S.; Saltiel, A.; Sawyer, T. K. Design of peptidomimetic lignads for the $pp60^{src}$ SH2 domain. *Bioorg. Med. Chem.* **1997**, *5*, 41−47.

(22) Plummer, M. S.; Holland, D. R.; Shahripour, A.; Lunney, E. A.; Fergus, J. H.; Marks, J. S.; McConnell, P.; Mueller, W. T.; Sawyer, T. K. Design, Synthesis, and Cocrystal Structure of a Nonpeptide Src SH2 Domain Ligand. *J. Med. Chem.* **1997**, *40*, 3719−3725.

(23) Charifson, P. S.; Shewchuk, L. M.; Rocque, W.; Hummel, C. W.; Jordan, S. R.; Mohr, C.; Pacofsky, G. J.; Peel, M. R.; Rodriguez, M.; Sternbach, D. D.; Consler, T. G. Peptide ligands of $pp60^{c-src}$ SH2 domains: A thermodynamic and structural study. *Biochemistry* **1997**, *36*, 6283−6293.

(24) Pacofsky, G. J.; Lackey, K.; Alligood, K. J.; Berman, J.; Charifson, P. S.; Crosby, R. M.; Dorsey, G. F.; Feldman, P. L.; Gilmer, T. M.; Hummel, C. W.; Jordan, S. R.; Mohr, C.; Rodriguez, M.; Shewchuk, L. M.; Sternbach, D. D. Potent dipeptide inhibitors of the pp60c-src SH2 domain. *J. Med. Chem.* **1998**, *41*, 1894−1908.

(25) Garcia-Echeverria, C.; Furet, P.; Gay, B.; Fretz, H.; Rahuel, J.; Schoepfer, J.; Caravatti, G. Potent Antagonists of the SH2 Domain of Grb2: Optimization of the X+1 Position of 3-Amino-Z-Tyr(PO3H2)-X+1-Asn-NH2. *J. Med. Chem.* **1998**, *41*, 1741−1744.

(26) Ramalingam, K.; Eaton, S. R.; Cody, W. L.; Lu, G. H.; Panek, R. L.; Waite, L. A.; Decker, S. J.; Keiser, J. A.; Doherty, A. M. Structure−activity studies of phosphorylated peptide inhibitors of the association of phosphatidylinositol 3-kinase with PDGF-β receptor. *Bioorg. Med. Chem.* **1995**, *3*, 1263−1272.

(27) Eaton, S. R.; Ramalingam, K.; Cody, W. L.; Holland, D. R.; Panek, R. L.; Lu, G. H.; Doherty, A. M. Structure−activity relationships of peptides that block the association of PDGF β-receptor with phosphatidylinositol 3-kinase. In *Peptides: Chemistry, Structure and Biology. Proceedings of the Fourteenth American Peptide Symposium;* Kaumaya, P. T. P., Hodges, R. S., Eds.; Mayflower Scientific Ltd.: West Midlands, England, 1996; pp 414−415.

(28) Cody, W. L.; Eaton, S. R.; Kent, D. R.; Panek, R. L.; Lu, G. H.; Dahring, T. K.; Doherty, A. M. The design of peptidomimetic inhibitors of the association of PDGF-β receptor and PI 3-kinase with cellular activity. In *Peptides 1996: Proceedings of the Twenty-Fourth European Peptide Symposium*; Ramage, R., Epton, R., Eds.; Mayflower Scientific Ltd.: West Midlands, England, 1998; pp 307−308.

(29) Waskman, G.; Shoelson, S. E.; Pant, N.; Cowburn, D.; Kuriyan, J. Binding of a high affinity phosphotyrosyl peptide to the src SH2 domain: Crystal structures of the complexed and peptide-free forms. *Cell* **1993**, *72*, 779−790.

(30) Eck, M. J.; Shoelson, S. E.; Harrison, S. C. Recognition of a high-affinity phosphotyrosyl peptde by the src homology-2 domain of $p56^{lck}$. *Nature* **1993**, *362*, 87−91.

(31) Nolte, R. T.; Eck, M. J.; Schlessinger, J.; Shoelson, S. E.; Harrison, S. C. Crystal structure of the PI 3-kinase p85 amino-terminal SH2 domain and its phosphopeptide complexes. *Nature Struct. Biol.* **1996**, *3*, 364−373.

(32) Weston, S.; Derbyshire, D.; Breeze, A.; Pauptit, R. 1.7 Å Structure of the C-terminal SH2 domain of the p85 subunit of human phosphatidylinositol 3-kinase. *Abstracts of Papers*; International Union of Crystallography, IUCr XVII: Seattle, WA, 1996; Abstract PS04.10.26.

(33) Breeze, A. L.; Kara, B. V.; Barratt, D. G.; Anderson, M.; Smith, J. C.; Luke, R. W.; Best, J. R.; Cartlidge, S. A. Structure of a specific peptide complex of the carboxy-terminal SH2 domain from the p85 alpha subunit of phosphatidylinositol 3-kinase. *EMBO J.* **1996**, *15*, 3579−3589.

(34) Hensmann, M.; Booker, G. W.; Panayotou, G.; Boyd, J.; Linacre, J.; Waterfield, M.; Campbell, I. D. Phosphopeptide binding to the N-terminal SH2 domain of the p85α subunit pf PI 3-kinase: A heteronuclear NMR study. *Protein Sci.* **1994**, *3*, 1020−1030.

(35) Roller, P. P.; Otaka, A.; Nomizu, M.; Smyth, M. S.; Barchi, J. J.; Burke, T. R.; Case, R. D.; Wolf, G.; Shoelson, S. E. Norleucine as a replacement for methionine in phosphatase-resistant linear and cyclic peptides which bind to p85 SH2 domains. *Bioorg. Med. Chem. Lett.* **1994**, *4*, 1879−1872.

(36) Stankovic, C. J.; Plummer, M. S.; Sawyer, T. K. Peptidomimetic ligands for src homolgy-2 domains. In *Advances in Amino Acid Mimetics and Peptidomimetics*; Abell, A., Ed.; Jai Press: Greenwich, CT, 1997; Vol. 1, pp 127−163.

(37) Zuckermann, R. N.; Kerr, J. M.; Kent, S. B. H.; Moos, W. H. Efficient method for the preparation of peptoids [oligo(N-substituted glycines)] by submonomer solid-phase synthesis. *J. Am. Chem. Soc.* **1992**, *114*, 10646−10647.

(38) Rink, H. Solid-phase synthesis of protected peptide fragments using a trialkoxy-diphenyl methyl ester resin. *Tetrahedron Lett.* **1987**, *28*, 3787−3790.

(39) Bernatowicz, M. S.; Daniels, S. B.; Koster, H. A comparison of acid-labile linkage agents for the synthesis of peptide C-terminal amides. *Tetrahedron Lett.* **1989**, *30*, 4645−4648.

(40) Mergler, M.; Tanner, R.; Gosteli, J.; Grogg, P. Peptide synthesis by a combination of solid-phase and solution methods. I. A new very acid-labile anchor group for the solid phase synthesis of fully protected fragments. *Tetrahedron Lett.* **1988**, *29*, 4005−4008.

(41) Mergler, M.; Nyfeler, R.; Tanner, R.; Gosteli, J.; Grogg, P. Peptide synthesis by a combination of solid-phase and solution methods. II. Synthesis of fully protected peptide fragments on 2-methoxy-4-alkoxybenzyl alcohol resin. *Tetrahedron Lett.* **1988**, *29*, 4009−4012.

(42) Carpino, L. A.; El-Faham, A.; Albericio, F. Racemization studies during solid-phase peptide synthesis using azabenzotriazole-based coupling reagents. *Tetrahedron Lett.* **1994**, *35*, 2279−2282.

(43) S. R. Eaton and W. L. Cody, Parke-Davis Pharmaceutical Research, Division of Warner-Lambert Co., unpublished results.

(44) Burke, T. R.; Smyth, M. S.; Otaka, A.; Nomizu, M.; Roller, P. P.; Wolf, G.; Case, R.; Shoelson, S. E. Nonhydrolyzable phosphotyrosyl mimetics for the preparation of phosphatase-resistant SH2 domain inhibitors. *Biochemistry* **1994**, *33*, 6490−6494.

(45) Gilmer, T.; Rodriguez, M.; Jordan, S.; Crosby, R.; Alligood, K.; Green, M.; Kimery, M.; Wagner, C.; Kinder, D.; Charifson, P.; Hassell, A. M.; Willard, D.; Luther, M.; Rusnak, D.; Sternbach, D. D.; Mehrotra, M.; Peel, M.; Shampine, L.; Davis, R.; Robbins, J.; Patel, I. R.; Kassel, D.; Burkhart, W.; Moyer, M.; Bradshaw, T.; Berman, J. Peptide inhibitors of src SH3-SH2-phosphoprotein interactions. *J. Biol. Chem.* **1994**, *269*, 31711−31719.

(46) Burke, T. R.; Nomizu, M.; Otaka, A.; Smyth, M. S.; Roller, P. P.; Case, R. D.; Wolf, G.; Shoelson, S. E. Cyclic peptide inhibitors of phosphatidylinositol 3-kinase p85 SH2 domain binding. *Biochem. Biophys. Res. Commun.* **1994**, *201*, 1148−1153.

(47) Burke, T. R.; Kole, H. K.; Roller, P. P. Potent inhibition of insulin receptor dephosphorylation by a hexamer peptide containing the phosphotyrosyl mimetic F2Pmp. *Biochem. Biophys. Res. Commun.* **1994**, *204*, 129−134.

(48) Stankovic, C. J.; Surendran, N.; Lunney, E. A.; Plummer, M. S.; Para, K. S.; Shahripour, A.; Fergus, J. H.; Marks, J. S.; Herrera, R.; Hubbell, S. E.; Humblet, C.; Saltiel, A. R.; Stewart, B. H.; Sawyer, T. K. The role of 4-phosphonodifluoromethyl- and 4-phosphono-phenylalanine in the selectivity and cellular uptake of SH2 domain ligands. *Bioorg. Med. Chem. Lett.* **1997**, *7*, 1909−1914.

(49) Rose, D. W.; Saltiel, A. L.; Majumdar, M.; Olefsky, J. M. IRS-1 is required for insulin-mediated mitogenic signal transduction. *Proc. Natl. Acad. Sci. U.S.A.* **1994**, *91*, 797−801.

(50) Morris, A. J.; Haruta, T.; Martin, S. S.; Ricketts, W. R.; Gustafson, T.; Rose, D. W.; Olefsky, J. M. Evidence for an insulin receptor substrate 1 independent insulin signaling pathway that mediates insulin-responsive glucose transporter (GLUT4) translocation. *Proc. Natl. Acad. Sci. U.S.A.* **1996**, *93*, 8401−8406.

(51) Jhun, B. H.; Rose, D. W.; Seely, B. L.; Saltiel, A. L.; Cantley, L.; Olefsky, J. M. Microinjection of the SH2 domain of the 85 kDa subunit of phosphatidylinositol 3-kinase inhibits insulin-induced DNA synthesis and c-fos expression. *Mol. Cell. Biol.* **1994**, *14*, 7466−7475.

(52) Martin, S. S.; Rose, D. W.; Klippel, A.; Williams, L. T.; Olefsky, J. M. Phosphatidylinositol 3-kinase is necessary and sufficient for insulin-stimulated stress fiber breakdown. *Endocrinology* **1996**, *137*, 5045−5054.

(53) Haruta, T.; Morris, A. J.; Rose, D. W.; Nelson, J. G.; Mueckler, M.; Olefsky, J. M. Insulin stimulated GLUT4 translocation is mediated by a divergent intracellular signaling pathway. *J. Biol. Chem.* **1995**, *270*, 27991−27994.

(54) Kari, U. P.; Maddukuri, S. R.; MacDonald, M. T.; Jones, L. M.; MacDonald, D. L.; Maloy, W. L. Structure−activity relationship studies of dialkylamine derivatives exhibiting wide spectrum of antimicrobial activities. *Program & Abstracts, Fifteenth American Peptide Symposium, Nashville, TN*; American Peptide Society: Minneapolis, MN, 1997; P0005.

(55) Yokum, T. S.; Elzer, P. H.; McLaughlin, M. L. Antimicrobial α,α-dialkylated amino acid rich peptides with in-vivo activity against an intracellular pathogen. *J. Med. Chem.* **1996**, *39*, 3603−3605.

(56) Wang, S. S. p-Alkoxybenzyl alcohol resin and p-alkoxybenzyl-carbonylhydrazide resin for solid-phase synthesis of protected peptide fragments. *J. Am. Chem. Soc.* **1973**, *95*, 1328−1333.

(57) Smyth, M. S.; Burke, T. R. Enantioselective synthesis of N-Boc and N-Fmoc protected diethyl 4-phosphono(difluoromethyl)-L-phenylalanine; agents suitable of the solid-phase synthesis of peptides containing nonhydrolyzable analogues of O-phosphotyrosine. *Tetrahedron Lett.* **1994**, *35*, 551−554.

(58) Stewart, J. M.; Young, J. D. *Solid-Phase Peptide Synthesis*, 2nd ed.; Pierce Chemical Co.: Rockford, IL, 1984.

(59) Fields, G. B.; Noble, R. L. Solid-phase peptide synthesis utilizing 9-fluorenylmethoxycarbonyl amino acids. *Int. J. Pept. Protein Res.* **1990**, *35*, 161−214.

(60) King, D. S.; Fields, C. G.; Fields, G. B. A cleavage method which minimizes side reactions following Fmoc solid-phase peptide synthesis. *Int. J. Pept. Protein Res.* **1990**, *36*, 255−266.

(61) Kitas, E. A.; Knorr, R.; Trzeciak, A.; Bannwarth, W. Alternative strategies for the Fmoc solid-phase synthesis of O-4-phospho-L-tyrosine-containing peptides. *Helv. Chim. Acta* **1991**, *74*, 1314−1328.

(62) Otaka, A.; Burke, T. R.; Smyth, M. S.; Nomizu, M.; Roller, P. P. Deprotection and cleavage methods for protected peptide resins containing 4-[(diethylphosphono)difluoromethyl]-DL-phenylalanine residues. *Tetrahedron Lett.* **1993**, *34*, 7039−7042.

(63) Sybyl, molecular modeling software version 6.0 ver. 1.0; Tripos Inc., St. Louis, MO; 1994.

(64) Lee, C. H.; Kominos, D.; Jacques, S.; Margolis, B.; Schlessinger, J.; Shoelson, S. E.; Kuriyan, J. Crystal structures of peptide complexes of the amino-terminal SH2 domain of the Syp tyrosine phosphatase. *Structure* **1994**, *2*, 423−425.

(65) Booker, G. W.; Breeze, A. L.; Downing, A. K.; Panayotou, G.; Gout, I.; Waterfield, M. D.; Campbell, I. D. Structure of an SH2 domain of the p85 α subunit of phosphatidylinositol-3-OH kinase. *Nature* **1992**, *358*, 684−687.

(66) Pascal, S. M.; Singer, A. U.; Gish, G.; Yamazaki, T.; Shoelson, S. E.; Pawson, T.; Kay, L. E.; Forman-Kay, J. D. Nuclear magnetic resonance structure of an SH2 domain of phospholiphase C-g1 complexed with a high affinity binding peptide. *Cell* **1994**, *77*, 461−472.

(67) Zhu, G.; Decker, S. J.; Mayer, B. J.; Saltiel, A. R. Direct analysis of the binding of the abl src homology 2 domain to the activated epidermal growth factor receptor. *J. Biol. Chem.* **1993**, *268*, 1775−1779.

(68) McClain, D. A.; Maegawa, H.; Lee, J.; Dull, T. J.; Ullrich, A.; Olefsky, J. M. A mutant insulin receptor with defective tyrosine kinase displays no biologic activity and does not undergo endocytosis. *J. Biol. Chem.* **1987**, *262*, 14663−14671.

(69) Xiao, S.; Rose, D. W.; Sasaoka, T.; Maegawa, H.; Burke, T. R.; Roller, P.; Shoelson, S. E.; Olefsky, J. M. Syp (SH-PTP2) is a positive mediator of growth factor stimulated mitogenic signal transduction. *J. Biol. Chem.* **1994**, *269*, 21244−21248.

(70) Kolch, W.; Philipp, A.; Mischak, H.; Dutil, E. M.; Mullen, T. M.; Meinkoth, J. M.; Feramisco, J. R.; Rose, D. W. Inhibition of Raf-1 signaling by a monoclonal antibody which interferes with Raf-1 activation and with Mek substrate binding. *Oncogene* **1996**, *13*, 1305−1314.

(71) Nicholls, A.; Sharp, K. A.; Honig, B. Protein folding and association: Insights from the interfactial and thermodynamic properties of hydrocarbons. *Proteins* **1991**, *11*, 281−296.

JM9802766